



HAL
open science

The fate of C 4 and C 3 macrophyte carbon in central Amazon floodplain waters: insights from a batch experiment

J.M. Mortillaro, C. Passarelli, G. Abril, C. Hubas, Patrick Albéric, L.F. Artigas, M.F. Benedetti, N. Thiney, P. Moreira-Turcq, M.A.P. Perez, et al.

► To cite this version:

J.M. Mortillaro, C. Passarelli, G. Abril, C. Hubas, Patrick Albéric, et al.. The fate of C 4 and C 3 macrophyte carbon in central Amazon floodplain waters: insights from a batch experiment. *Limnologia*, 2016, 59, pp.90-98. 10.1016/j.limno.2016.03.008 . insu-01321951

HAL Id: insu-01321951

<https://insu.hal.science/insu-01321951>

Submitted on 30 May 2016

HAL is a multi-disciplinary open access archive for the deposit and dissemination of scientific research documents, whether they are published or not. The documents may come from teaching and research institutions in France or abroad, or from public or private research centers.

L'archive ouverte pluridisciplinaire **HAL**, est destinée au dépôt et à la diffusion de documents scientifiques de niveau recherche, publiés ou non, émanant des établissements d'enseignement et de recherche français ou étrangers, des laboratoires publics ou privés.



Distributed under a Creative Commons Attribution - NonCommercial - ShareAlike 4.0 International License

Accepted Manuscript

Title: The fate of C₄ and C₃ macrophyte carbon in central Amazon floodplain waters: insights from a batch experiment

Author: J.M. Mortillaro C. Passarelli G. Abril C. Hubas P. Alberic L.F. Artigas M.F. Benedetti N. Thiney P. Moreira-Turcq M. Perez L.O. Vidal T. Meziane



PII: S0075-9511(16)30022-6
DOI: <http://dx.doi.org/doi:10.1016/j.limno.2016.03.008>
Reference: LIMNO 25510

To appear in:

Received date: 15-5-2015
Revised date: 1-3-2016
Accepted date: 6-3-2016

Please cite this article as: Mortillaro, J.M., Passarelli, C., Abril, G., Hubas, C., Alberic, P., Artigas, L.F., Benedetti, M.F., Thiney, N., Moreira-Turcq, P., Perez, M., Vidal, L.O., Meziane, T., The fate of C₄ and C₃ macrophyte carbon in central Amazon floodplain waters: insights from a batch experiment. *Limnologia* <http://dx.doi.org/10.1016/j.limno.2016.03.008>

This is a PDF file of an unedited manuscript that has been accepted for publication. As a service to our customers we are providing this early version of the manuscript. The manuscript will undergo copyediting, typesetting, and review of the resulting proof before it is published in its final form. Please note that during the production process errors may be discovered which could affect the content, and all legal disclaimers that apply to the journal pertain.

The fate of C₄ and C₃ macrophyte carbon in central Amazon floodplain waters: insights from a batch experiment

J.M. Mortillaro^{1*}, C. Passarelli¹, G. Abril^{2,3}, C. Hubas¹, P. Alberic⁴, L.F. Artigas⁵, M.F. Benedetti⁶, N. Thiney¹, P. Moreira-Turcq⁷, M. Perez^{3,6}, L.O. Vidal⁸, T. Meziane¹

1 Unité Mixte de Recherche Biologie des organismes et écosystèmes aquatiques (BOREA UMR 7208), Sorbonne Université, Muséum national d'Histoire naturelle, Université Pierre et Marie Curie, Université de Caen Basse-Normandie, CNRS, IRD, CP53, 61 rue Buffon 75005 Paris, France

2 Laboratoire Environnement et Paléoenvironnements Océanique (EPOC) UMR-CNRS 5805, Université de Bordeaux, Allée Geoffroy Saint-Hilaire 33615 Pessac, France

3 Universidade Federal Fluminense, Department of Geochemistry, Niteroi, Rio de Janeiro, Brazil

4 Institut des Sciences de la Terre d'Orléans, 1A rue de la Férollerie, 45071 Orléans Cedex 2, France

5 Laboratoire d'Océanologie et Géosciences (LOG), UMR-CNRS-ULCO-UL1 8187, Université du Littoral Côte d'Opale (ULCO), 32 avenue Foch, 62930 Wimereux, France

6 Equipe Géochimie des Eaux, Institut de Physique du Globe de Paris, Université Paris Diderot, Sorbonne Paris Cité, 35 rue Hélène Brion, 75205 Paris Cedex 13, France

7 Institut de Recherche pour le Développement, 32 avenue Henri Varagnat, 93143 Bondy, France

8 Laboratório de Ecologia Aquática, Departamento de Biologia, Universidade Federal de Juiz de Fora, Rua José Lourenço Kelmer, MG 36036-900 Juiz de Fora, Brazil

* Corresponding author: Tel: +33 4 6761 4467

E-mail: jean-michel.mortillaro@cirad.fr

Abbreviated title: Degradation of central Amazon macrophytes

Keywords: Central Amazon, floodplains, fatty acids, stable isotopes, macrophytes, degradation

1 **Summary**

2 The central Amazon floodplains are particularly productive ecosystems, where a large
3 diversity of organic carbon sources are available for aquatic organisms. Despite the fact that
4 C₄ macrophytes generally produce larger biomasses than C₃ macrophytes, food webs in the
5 central Amazon floodplains appear dominantly based on a C₃ carbon source.

6 In order to investigate the respective fate and degradation patterns of C₄ and C₃ aquatic plant-
7 derived material in central Amazon floodplains, we developed a 23-days batch experiment.

8 Fatty acid and carbon concentrations as well as stable isotope compositions were monitored
9 over time in 60 L tanks. These tanks contained Amazon water, with different biomasses of C₃
10 and C₄ macrophyte, representative of *in situ* densities occurring in central Amazon
11 floodplains.

12 In the C₄ *Paspalum repens* treatments, organic (POC, DOC) and inorganic carbon (DIC) got
13 rapidly enriched in ¹³C, whereas in the C₃ *Salvinia auriculata* treatments, POC and DOC
14 showed little change in concentration and isotopic composition, and DIC got depleted in ¹³C.
15 The contribution of *P. repens* to POC and DOC was estimated to reach up to 94.2 and 70.7 %,
16 respectively. In contrast, no differences were reported between the C₃ *S. auriculata* and
17 control treatments, an observation attributed to the lower C₃ biomass encountered in the field,
18 to a slower degradation rate of C₃ compared to C₄ compounds, and to similar isotopic
19 compositions for river POC and DOC, and C₃ compounds.

20 The ¹³C enrichments of POC, DOC, and DIC from *P. repens* treatments were attributed to an
21 enhanced bacterially-mediated hydrolysis and mineralization of C₄ material. Evolutions of
22 bacterial abundance and branched fatty acid concentrations confirmed the role of
23 heterotrophic microbial communities in the high *P. repens* decomposition rate. Our
24 experiment highlights the predominant role of C₄ aquatic plants, as a large source of almost
25 entirely biodegradable organic matter available for heterotrophic activity and CO₂ outgassing
26 to the atmosphere.

27

27

28 **Introduction**

29 One of the largest sources of organic carbon in Amazon floodplains is derived from aquatic
30 macrophytes, which contribute up to half of the ecosystem primary production (Melack &
31 Forsberg, 2001). These macrophytes grow emerged, submerged or floating, with 388 species
32 described in a várzea (i.e. white-water nutrient rich floodplain) located near the city of
33 Manaus, in central Amazon (Junk & Piedade, 1993b). Among the most abundant species, the
34 floating grasses *Echinochloa polystachya* and *Paspalum fasciculatum* (Poaceae family) can
35 reach biomasses of 80 and 60 t ha⁻¹, respectively (Junk & Piedade, 1993a; Piedade et al.,
36 1991). Another macrophyte largely represented in the várzea is *P. repens* (up to 22 t ha⁻¹,
37 Fig. 1, Junk & Piedade, 1993a). These aerial species, which convert atmospheric carbon
38 dioxide into biomass through a C₄ pathway, constitute floating meadows that can extend over
39 large areas of floodplains (Junk & Howard-Williams, 1984; Hess et al., 2003; Silva et al.,
40 2013). Amazon floating meadows may also be composed of macrophytes using the C₃
41 photosynthetic pathway such as *Eichhornia* sp., *Pistia stratiotes* and *Salvinia auriculata*
42 (Fig. 1). However, the biomass of all these C₃ macrophytes add up to 3 to 15 t ha⁻¹ only
43 (Furch & Junk, 1992).

44 The ecology of C₃ and C₄ macrophytes, and particularly their biomass and production rates,
45 have been thoroughly examined (e.g. Morison et al., 2000; Engle et al., 2008; Silva et al.,
46 2013). Despite their large abundance, C₄ macrophytes constitute a minor source of energy for
47 Amazon aquatic food webs (Hamilton et al., 1992; Forsberg et al., 1993; Mortillaro et al.,
48 2015) and modest contributors to particulate organic carbon (POC, Hedges et al., 1986;
49 Mortillaro et al., 2011; Moreira-Turcq et al., 2013). Indeed, C₄ macrophytes are largely ¹³C
50 enriched (-12 ‰, Hedges et al., 1986; Mortillaro et al., 2011) compared to POC in rivers and
51 várzea of the Amazon (-30 ‰, Quay et al., 1992; Hedges et al., 1994). The almost constant
52 isotopic composition of dissolved organic carbon (DOC), at around -29 ‰ in the Amazon
53 River, suggests a dominant C₃ source such as terrestrial plants and/or macrophytes. In
54 contrast, dissolved inorganic carbon (DIC) is much heavier (-17.7 to -11.5 ‰, Quay et al.,
55 1992), i.e. closer to C₄ macrophytes signature, but also closer to the signature of atmospheric
56 CO₂. This isotopic composition results from isotopic equilibration induced by CO₂ gas
57 exchange (Quay et al., 1992; Hedges et al., 1994; Mayorga et al., 2005; Abril et al., 2014),
58 and/or due to carbonate mineral weathering (e.g. chemical or mechanical decay of rocks,
59 Mayorga et al., 2005).

60 Previous macrophyte (C₃ and C₄) degradation experiments in litterbags, exposed to natural
61 weathering, found an initially rapid loss of weight and a decrease in nutrients
62 (Howard-Williams & Junk, 1976; Furch & Junk, 1992). However, the contribution of
63 macrophytes to the Amazon aquatic food webs was not verified by Fellerhoff et al. (2003) in
64 their degradation experiment. Therefore, in order to examine the apparent discrepancy
65 between the high biomass of C₄ macrophytes in the floodplains and their modest contribution
66 to the organic matter (OM) pool in the Amazon river-floodplain ecosystem, a degradation
67 experiment was designed to investigate the fate of carbon from C₄ and C₃ macrophytes in
68 microcosms. Particulate and dissolved carbon concentrations, stable isotope compositions and
69 fatty acids (FA) concentrations, were analyzed in large volumes of Amazon waters incubated
70 with variable amounts of a C₄ and a C₃ macrophyte. Bacterial abundance and nutrient
71 concentrations complemented the description of macrophyte degradation throughout a 23-day
72 experiment. Our work hypothesis was that very fast decomposition and mineralization of C₄
73 macrophytes explain their low contribution to central Amazon aquatic food webs.

74

75 **Material and methods**

76 *Sampling*

77 In order to follow the fate of OM during the degradation of two aquatic macrophytes and the
78 influence of degradation products on the quality of POM, samples of *P. repens* (C₄) and
79 *S. auriculata* (C₃, Fig. 1) were collected in the Camaleão Lake (várzea), located by the
80 Solimões River. These two macrophytes were selected for their widespread distribution in
81 central Amazon floodplains and their large FA concentration compared to other macrophyte
82 species (i.e. *Eichhornia* sp. and *Pistia stratiotes*), as characterized in a previous study
83 (Mortillaro et al., 2011).

84 Macrophyte samples were sorted in order to eliminate dead leaves and washed to remove
85 sediment and invertebrates. About 900 L of water were also sampled from the lake and
86 distributed into 15 microcosms of 60 L each. Three water samples and three portions of each
87 macrophyte were collected in order to get their initial composition (i.e. stable isotopes and
88 FA).

89 *Experimental setup*

90 The experiment was implemented on the *Yane José IV* boat in August-September 2010. Five
91 experimental treatments were used: high and low biomasses of *P. repens* (PR-HB and PR-LB,
92 respectively) and *S. auriculata* (SA-HB and SA-LB, respectively), as well as a control

93 without macrophyte (Ctrl). These five treatments were selected to distinguish species effect
94 from biomass effect on water characterization. For each treatment, triplicate microcosms were
95 used. In PR-HB microcosms, 250 g of fresh *P. repens* leaves (25.6 gC) were used. This
96 amount was estimated from a maximum dry biomass of 22 t ha⁻¹ (recorded in the Januári
97 Lake near Camaleão Lake, Junk & Piedade, 1993a), with less than one fifth of emerged
98 *P. repens* biomass (Silva et al., 2009), an estimated water proportion of 75.9 % and a
99 microcosms surface of 0.13 m². Similarly, the mean *S. auriculata* dry biomass was estimated
100 to be 1 t ha⁻¹ (Junk & Piedade, 1997) giving a theoretical wet weight of 200 g (93.5 % of
101 water). However, low biomasses of *S. auriculata* were available during sampling, so that only
102 100 g (2.3 gC) per microcosm were used (SA-HB). Low biomass treatments contained 10 %
103 of the high biomass amount for each species (25 g of macrophytes for PR-LB and 10 g for
104 SA-LB). Macrophyte leaves were introduced into microcosms filled with floodplain water,
105 and were kept in the dark under constant temperature conditions (28 °C). Permanent stirring
106 with a water pump ensured oxygenation of the microcosms (from 40 to 100 % air-saturation)
107 and avoided anaerobic conditions to occur. Although low dissolved oxygen is common under
108 floating macrophytes in várzea (~50 % saturation, Engle & Melack, 1993), permanent
109 oxygenation was maintained in order to match natural conditions within floating meadows in
110 open waters, where wind and water currents are sufficient to maintain aerated to hypoxic
111 waters (30 % min) in 2-6 meter depth water column (Vidal et al., 2015).
112 In each treatment, samples were collected after 3, 6, 12, 18 and 23 days of experiment. At
113 each sampling time, around 3.5 L of water were collected and pre-filtered on 200 µm to avoid
114 heterogeneity between samples due to contamination with macrophyte fragments.
115 Consequently, POC concentrations reported here concern the fraction smaller than 200 µm.
116 Microcosms volume (60 L) was chosen so that at the end of the experiment, 70 % of the
117 initial water volume was still available, to avoid any concentration bias in the course of the
118 experiment.

119 *Sample analyses*

120 The FA compositions of POM and macrophytes were analyzed with a gas chromatograph
121 (Varian CP-3800 with flame ionization detector) after extraction, following a modified
122 method of Bligh & Dyer (1959) as described in Mortillaro et al. (2011). POM samples were
123 obtained after immediate on-board filtration (GF/F, 0.7 µm, pre-combusted 12 h at 450 °C)
124 using a vacuum system under low pressure, after which filters were freeze dried and stored at
125 -20 °C until analysis. The carbon and nitrogen compositions, and isotopic ratio (¹³C/¹²C or
126 ¹⁵N/¹⁴N), of dried POM and macrophyte samples were determined at the UC Davis Stable

127 Isotope Facility and reported in standard delta notation ($\delta^{13}\text{C}$ or $\delta^{15}\text{N}$), defined as parts per
128 thousand (‰) deviation from a standard (Vienna PeeDee Belemnite for $\delta^{13}\text{C}$ and atmospheric
129 N_2 for $\delta^{15}\text{N}$, Peterson & Fry, 1987). The DOC concentrations and isotopic compositions
130 ($\delta^{13}\text{C}$ -DOC) were determined using an EA-IRMS analyzer following the protocol of Alberic
131 (2011). The DIC isotopic compositions ($\delta^{13}\text{C}$ -DIC) were also determined using an EA-IRMS
132 analyzer following the protocol of Bouillon et al. (2007). However, DIC concentrations were
133 not measured, as microcosms were continuously aerated with pumps. The concentration of
134 nitrites (NO_2^-), nitrates (NO_3^-) and ammonium (NH_4^+) dissolved fractions, summarized as
135 DIN (dissolved inorganic nitrogen), as well as orthophosphate concentrations (PO_4^{3-}) were
136 determined by spectrophotometry following a modified method of Grasshoff (1999). Total
137 bacterial abundances were determined by direct epifluorescence microscopy counting, using
138 4,6-diamidino-2-phenyl-indole (DAPI) up to a final concentration of $1 \mu\text{g mL}^{-1}$ after 15 min
139 of incubation (Porter & Feig, 1980). Direct counts were performed at 1 250x magnification,
140 under an epifluorescence microscope (Leica Leitz DMR; 365 nm). In turbid samples (high
141 suspended matter content), subsamples were pre-treated (before staining) by addition of
142 150 μl of Tween, sonicated at 35 khz for 5 min, and centrifuged at 3 000 g during 10 min at
143 4°C (Chevaldonne & Godfroy, 1997; Hubas et al., 2007a, 2007b).

144 *Data analysis*

145 The data obtained for each microcosm were compared, to evidence variations between
146 treatments. All FA of POM (up to 40) were used in these analyzes without transformation and
147 were represented by their relative proportions. A dissimilarity matrix between each pair of
148 samples was calculated using the Bray-Curtis index. Dissimilarities between samples were
149 then graphically represented using an nMDS (non-metric MultiDimensional Scaling, Zuur et
150 al., 2007). Differences between groups were tested using analyzes of similarities tests
151 (ANOSIM, Oksanen et al., 2010), without considering temporal variability. When differences
152 were significant, a similarity percentages analysis (SIMPER, Oksanen et al., 2010) was used
153 to determine the relative contribution of each FA to differences between two groups.
154 The differences in the isotopic compositions ($\delta^{13}\text{C}$ -DOC, $\delta^{13}\text{C}$ -POC, $\delta^{15}\text{N}$ -PON and
155 $\delta^{13}\text{C}$ -DIC) as well as differences in POC, DOC, DIN, PO_4^{3-} concentrations and bacterial
156 abundance between treatments ($n = 5$) were tested using a non-parametric Kruskal-Wallis test
157 (KW). Non-parametric Mann-Whitney-Wilcoxon (MWW) Post-Hoc tests were then used to
158 identify the differences between individual treatments, after correction following a Benjamini
159 and Hochberg (BH) procedure for multiple comparisons (Benjamini & Hochberg, 1995).

160 The relative contribution of C_4 macrophytes to POM was calculated using a two end member
 161 mixing model (Forsberg et al., 1993):

$$162 \quad \%C_4 = \left[1 - \frac{\delta^{13}C_{source} - \delta^{13}C_{C_4}}{\delta^{13}C_{T_0} - \delta^{13}C_{C_4}} \right] \times 100 \quad (\text{Eq. 1})$$

163 where $\delta^{13}C_{source}$ was the $\delta^{13}C$ -POC compositions for each time and treatment, $\delta^{13}C_{C_4}$ was the
 164 mean *P. repens* composition, $\delta^{13}C_{T_0}$ was the mean POM composition at the beginning of the
 165 experiment and % C_4 the *P. repens* contribution to the isotopic compositions of OM in each
 166 sample.

167 All statistical analyzes were implemented within the R programming environment (R
 168 Development Core Team 2010, package Vegan, Oksanen et al., 2010), with the probability α
 169 set at 0.05.

170

171 **Results**

172 Among macrophyte samples, 41 FA were identified (Table 1) with an intragroup similarity of
 173 92.5 and 93.2 % within *P. repens* and *S. auriculata*, respectively, at the beginning of the
 174 experiment. *P. repens* was ^{13}C and ^{15}N enriched compared to *S. auriculata* (Table 1).

175 The water collected in the várzea was characterized by 37 FA (Table 1), where saturated 14:0,
 176 15:0, 16:0 and 18:0 accounted for 70 % of the total FA composition of POM. The POC and
 177 DOC concentrations were respectively of 1.3 ± 0.1 and 2.8 ± 0.3 mg L⁻¹ (Fig. 3), with a
 178 carbon isotopic composition of -30.1 ± 0.4 ‰ for POC and -28.7 ± 0.4 ‰ for DOC (Fig. 4).
 179 DIC was ^{13}C enriched relative to POC and DOC ($\delta^{13}C$ -DIC of -11.9 ± 0.2 ‰, Fig. 4).

180 Water from the five treatments showed significant differences in their global FA compositions
 181 (ANOSIM, $R = 0.35$, $p < 0.001$, Fig. 2). Samples from Ctrl, SA-LB, SA-HB, and PR-LB had
 182 a similar FA composition but differed from samples of PR-HB (Table 2). Similarities in the
 183 FA composition within each treatment were higher than 77 % (Table 3). A higher proportion
 184 of branched FA (mainly 15:0iso and 15:0anteiso) and a lower proportion of 18:0 were
 185 observed in PR-HB compared to other treatments (Table 3). The concentrations of POC,
 186 DOC, DIN, PO_4^{3-} as well as $\delta^{13}C$ -POC, $\delta^{13}C$ -DOC, $\delta^{13}C$ -DIC and bacterial abundance
 187 displayed significant differences between treatments (KW, $p < 0.001$, Table 4, Figs. 3-5),
 188 whereas $\delta^{15}N$ -PON was similar between all treatments (KW, $p = 0.73$).

189 The highest concentrations of POC, DOC, DIN, PO_4^{3-} and highest bacterial abundance, were
 190 observed in PR-HB (Figs. 3 & 5, Table 4). However, a higher POC concentration was

191 recorded in SA-HB compared to PR-LB and SA-LB (Table 4, Fig. 3). No differences in DOC
192 concentration were observed between SA-HB, PR-LB and Ctrl, whereas SA-LB displayed the
193 lowest DOC concentration. In contrast, the $\delta^{13}\text{C}$ -POC was significantly higher in PR-HB
194 ($-14.3 \pm 1.0 \text{ ‰}$) and in PR-LB ($-21.0 \pm 3.1 \text{ ‰}$) compared to other treatments (Fig. 4, Table 4).
195 However, no difference was found between the isotopic compositions of SA and Ctrl
196 treatments (MWW, $p > 0.05$, Table 4). The contribution of *P. repens* to the ^{13}C enrichment
197 recorded in POC from PR-HB and PR-LB reached 94.2 and 63.2 %, respectively (Fig. 4,
198 Eq. 1). Similarly, the highest $\delta^{13}\text{C}$ -DOC was recorded in PR-HB ($-17.8 \pm 1.2 \text{ ‰}$) with a
199 contribution of *P. repens* to the DOC of 70.7 % (Fig. 4, Eq. 1). A higher $\delta^{13}\text{C}$ -DOC was also
200 observed in PR-LB ($-24.9 \pm 1.0 \text{ ‰}$, Fig. 4, Table 4) compared to SA-HB and SA-LB, with a
201 contribution of *P. repens* to the DOC reaching 27.8 %. A significant increase in $\delta^{13}\text{C}$ -DIC was
202 only recorded for PR-HB ($-5.9 \pm 2.9 \text{ ‰}$, Fig. 4, Table 4), concomitantly to a decrease in
203 $\delta^{13}\text{C}$ -DIC for SA-HB ($-17.8 \pm 3.7 \text{ ‰}$, Fig. 4, Table 4). In contrast, no differences were found
204 between the Ctrl with both SA and PR low biomass treatments (MWW, $p > 0.05$, Table 4).
205 $\delta^{13}\text{C}$ of organic and inorganic matters increased after 3 to 6 days in PR treatments, whereas no
206 temporal trends were recorded for Ctrl and SA treatments except for $\delta^{13}\text{C}$ -DIC of SA-HB
207 (Fig. 4).

208

209 Discussion

210 The present microcosm experiment highlights significantly different degradation patterns of
211 two C_3 and C_4 Amazon macrophytes. Over a 23 day experiment, our results revealed a major
212 impact of *P. repens* degradation, at high biomass, on OM composition. This impact was
213 apparently related to the biomass of macrophytes used in the experiment as well as to the
214 inherent biodegradability of C_4 compared to C_3 macrophytes. Indeed, even though the fast
215 degradation of the C_4 macrophyte was most evident in PR-HB, as revealed by all measured
216 parameters, it was also observed in the PR-LB. For instance, PR-LB treatments (25 g of fresh
217 macrophytes in a 60 L tank) showed stronger ^{13}C enrichment in POC and DOC than SA-HB
218 (100 g of macrophytes in a 60 L tank). There was however a slight increase in POC
219 concentrations as well as a decrease in $\delta^{13}\text{C}$ -DIC in the *S. auriculata* high biomass treatments
220 that reveals on-going degradation.

221 In this experiment, *P. repens* displayed large proportions of 18:2 ω 6 and 18:3 ω 3
222 polyunsaturated FA (up to 44 % of total FA), which is consistent with previous
223 characterization of this FA as markers of macrophytes in this environment (Mortillaro et al.,

224 2011). Similarly, carbon stable isotope compositions of both *P. repens* and *S. auriculata* were
225 consistent with those expected from plants with C₄ and C₃ photosynthetic pathways
226 (-13.0 ± 0.8 and -30.5 ± 0.5 ‰, respectively, Smith & Epstein, 1971).

227 *Contribution of P. repens (C₄) and S. auriculata (C₃) to POM*

228 In PR treatments, POC was significantly enriched in ¹³C, which indicates a contribution of *P.*
229 *repens*, after its hydrolysis into the POM pool. This contribution was estimated to reach 94.2
230 and 63.2 % of total POM composition for PR-HB and PR-LB, respectively, using a two-end-
231 member mixing model. This was surprising as previous studies, characterizing POM in the
232 Amazon Basin, suggested a low contribution of C₄ macrophytes (Hedges et al., 1986;
233 Mortillaro et al., 2011; Moreira-Turcq et al., 2013). The contribution of *P. repens* to POM
234 was confirmed by the increased proportion of branched FA in PR treatments (15:0iso and
235 15:0anteiso). These FA are regularly described as biomarkers of bacteria (Volkman et al.,
236 1980; Kaneda, 1991; Mfilinge et al., 2003) and suggest here that in addition to hydrolysis,
237 *P. repens* leaves were decomposed by heterotrophic microbial communities. Indeed, the
238 transfer of FA to POM, including branched FA, was previously recorded from decomposing
239 mangroves (Mfilinge et al., 2003). Similarly, the transfer of FA and the ¹³C enrichment of
240 POM and sediments were evidenced in salt-marsh from the decomposition of the C₄ *Spartina*
241 spp. (Boschker et al., 1999). In salt-marsh ecosystems, the composition of POM affected by
242 *Spartina* spp. decomposition changed from predominantly unsaturated to branched and
243 saturated FA typical of bacteria (Johnson & Calder, 1973; Schultz & Quinn, 1973). Similar
244 findings were reported in PR-HB and differences in FA compositions and ¹³C enrichments
245 reported for OM between PR and Ctrl treatments occurred in the first 3 to 6 days of the
246 experiment. These changes in OM composition, as well as high bacterial abundance recorded
247 in PR-HB, suggest a fast decomposition of this macrophyte, which may have exceeded
248 hydrolysis (in agreement with previous studies; Fellerhoff et al., 2003).

249 Contrastingly to *P. repens*, no differences were reported between SA and Ctrl treatments for
250 FA and δ¹³C-POC. Yet, decomposition of *S. auriculata* could not be excluded using
251 δ¹³C-POC analyses. Indeed, fresh leaves of *S. auriculata* (-30.5 ± 0.5 ‰) had a similar
252 composition to POM (-30.1 ± 0.4 ‰) at the beginning of the experiment. However, the higher
253 POC concentrations measured in SA-HB compared to PR-LB and SA-LB suggest an effective
254 hydrolysis of this macrophyte. The lack of differences between SA and Ctrl treatments for FA
255 compositions and δ¹³C-POC suggest however a slower hydrolysis of *S. auriculata* compared
256 to *P. repens*. Indeed, Howard-Williams & Junk (1976) recovered 50 % of *S. auriculata* initial
257 dry weight at the end of a 186 days decomposition experiment. Similarly, Fellerhoff et al.

258 (2003) recovered 80 % of *S. auriculata* initial dry weight after 21 days of incubation. During
259 our experiment, large macrophyte debris were observed for a much longer time in the
260 *S. auriculata* treatments than in the *P. repens* treatments. This higher resistance to
261 fractionation of the C₃ macrophyte was consistent with the differences in FA, POC and
262 $\delta^{13}\text{C}$ -POC of the fine POM fraction (<200 μm).

263 *Impact of macrophyte degradation on dissolved compounds*

264 Decomposition of *P. repens* tissues led to a ^{13}C enrichment of DOC and DIC. Such increase
265 of $\delta^{13}\text{C}$ -DIC resulted from bacterial mineralization of macrophyte organic carbon and CO₂
266 equilibration at the air/water interface (Quay et al., 1992; Hedges et al., 1994; Mayorga et al.,
267 2005). Because the experiment was performed in contact with air in order to maintain aerobic
268 conditions, the $\delta^{13}\text{C}$ -DIC signature was affected by isotopic equilibration with the
269 atmosphere. This process tends to slowly increase the $\delta^{13}\text{C}$ -DIC to a value close to the
270 isotopic equilibrium with the atmosphere at around 0 ‰ (Polsenaere & Abril, 2012).
271 Consequently, the observed $\delta^{13}\text{C}$ -DIC values are the result of a balance between the DIC
272 production from the C₃ or C₄ plants decomposition and equilibration with the atmosphere. In
273 SA-HB, the rapid $\delta^{13}\text{C}$ -DIC decrease from -11.9 ± 0.2 ‰ at the beginning of the experiment
274 to -20.3 ± 7.0 ‰ after 3 days of incubation reveals that the C₃ macrophytes were undergoing
275 mineralization processes. Indeed, hydrolysis tends to leach out compounds relatively enriched
276 in ^{13}C with respect to more recalcitrant compounds (e.g. lignin) depleted in ^{13}C (Costantini et
277 al., 2014).

278 Previous works in the Amazon have attributed ^{13}C enrichment of DIC to the preferential
279 oxidation of organic carbon derived from C₄ macrophytes (Rai & Hill, 1984; Chanton et al.,
280 1989; Quay et al., 1992; Waichman, 1996). Several other studies based on solute distribution
281 suggested that C₄ grasses are more biodegradable than the bulk OM (Hedges et al., 1986;
282 Quay et al., 1992; Mayorga et al., 2005). Ellis et al. (2012) have measured the $\delta^{13}\text{C}$ of respired
283 CO₂ in closed incubations at different stages of the hydrological cycle in the Solimões River
284 and concluded that C₃ plants, C₄ plants and phytoplankton, all contributed to respiration in the
285 Amazon River. The results of our incubations suggest however that high macrophyte
286 biomasses are necessary in order to significantly alter the $\delta^{13}\text{C}$ -DIC signature locally.
287 Besides carbon, the nitrogen (N) and phosphorus (P) concentrations in floodplain waters were
288 also affected by the decomposition and mineralization of macrophytes. A large release of PO₄,
289 DIN and potassium (K) was previously evidenced during the decomposition of
290 *P. fasciculatum* (Furch & Junk, 1992). The decomposition of *P. fasciculatum* had the potential
291 to supply floodplains with 242 kg ha⁻¹ of N and 66 kg ha⁻¹ of P in Furch & Junk (1992)

292 nutrients budget. Following these authors' calculations (i.e. maximum amounts of bio-
293 elements released to water reported to maximum macrophyte biomasses), *P. repens* showed
294 the potential, in our degradation experiment, to supply floodplains with 176.4 kg ha⁻¹ of N and
295 48.2 kg ha⁻¹ of P. On the other hand, *S. auriculata* contribution to floodplains is estimated to
296 reach 0.13 kg ha⁻¹ of N and 2.44 kg ha⁻¹ of P only. Therefore, our study demonstrates that
297 *P. repens* represents a predominant source of N and P.

298 Fast nutrient recycling from decomposing macrophytes may fertilize Amazon floodplains,
299 where N and P are growth-limiting factors (Devol et al., 1984; Forsberg, 1984; Setaro &
300 Melack, 1984). Within the Amazon Basin, aquatic grasses such as *P. repens* have been
301 suggested to be able of atmospheric N₂ fixation (Martinelli et al., 1992), so that atmospheric
302 N₂ may contribute up to 90 % of plant N for stands of *P. repens* (Kern & Darwich, 2003).
303 Therefore, the fast decomposition of N₂ fixing macrophytes may play a predominant role as a
304 natural fertilizer for floodplains (Piedade et al., 1991; Kern & Darwich, 2003), stimulating
305 phytoplankton production during the falling water period, when macrophytes start to
306 decompose (Rai & Hill, 1984).

307 In Amazon floodplains, *P. repens* maximum biomasses were observed during the wet season
308 (Junk & Piedade, 1993b, Silva et al., 2009), where C₄ macrophyte contribution to the primary
309 production in várzea was estimated to reach 65 % (Melack & Forsberg, 2001). During this
310 season, POC and DOC mainly originate from depleted carbon sources similar to C₃ primary
311 producers (Hedges et al., 1994, Mortillaro et al., 2011). However during the dry season,
312 macrophytes are subject to intensive degradation as water level decreases (Engle et al., 2008).
313 An increasing contribution of macrophytes to OM composition, due to the accumulation of
314 plant detritus, was suggested in the Amazon várzea (Mortillaro et al., 2011). However,
315 although macrophytes have been demonstrated experimentally to affect the δ¹³C-POC and
316 δ¹³C-DOC, fast microbial mineralization of organic carbon suggests that only large
317 macrophyte biomasses, produced during the flood season, have the potential to affect
318 δ¹³C-POC and δ¹³C-DOC within floodplains. Indeed, C₄ material may contribute to sediments
319 OM composition (Sobrinho et al., 2016) according to spatial variability in C₄ macrophytes
320 (Hess et al., 2003), despite a low burial of organic carbon in floodplain sediments (Moreira-
321 Turcq et al., 2004). Therefore, most C₄ macrophytes are mineralized (Piedade et al., 1991;
322 Junk & Piedade, 1993a) and thus contribute significantly to CO₂ outgassing, as previously
323 suggested (Quay et al., 1992). Moreover, bacterial growth has been shown, within Amazon
324 floodplains, to display a low efficiency (Vidal et al., 2015). This low efficiency implies,
325 besides high respiration rates, a low transfer of C₄ carbon to higher trophic levels. The

326 production of C₃ macrophytes within the central Amazon Basin is much more limited than C₄
327 macrophytes (Furch & Junk, 1992). However, the lower lability of these macrophyte debris
328 compared to C₄ macrophyte debris makes them available for being channeled through aquatic
329 food webs. These findings can explain why Amazon food webs are mainly centered on a C₃
330 carbon source (Araujo-Lima et al., 1986; Hamilton et al., 1992; Forsberg et al., 1993),
331 although C₄ macrophytes display a greater food quality and biomass for specialized herbivore
332 fish species (Mortillaro et al., 2015).

333

334 **Conclusion**

335 Within the present experiment, the higher lability of C₄ compared to C₃ macrophytes was
336 demonstrated. The contribution of *P. repens* to POC and DOC isotopes compositions reached
337 a maximum after 3 to 6 days, indicating a fast decomposition rate of this macrophyte.
338 Moreover, *P. repens* biomasses had a noticeable impact on OM composition. The
339 decomposition of C₄ macrophytes was followed by the mineralization into DIC, as suggested
340 by $\delta^{13}\text{C}$ -DIC, as well as by the release of DIN and P. Therefore, the fast mineralization of C₄
341 macrophytes, as well as the natural mixing of POM with ¹³C-depleted primary producers (e.g.
342 phytoplankton, C₃ macrophytes, periphyton, and trees), should account for the overall low
343 contribution of C₄ carbon sources to the central Amazon aquatic food webs.

344

345 **Acknowledgments**

346 This research is a contribution to the CARBAMA project, supported by the ANR (French
347 National Agency for Research, grant number 08-BLAN-0221), and the CNPq (National
348 Council for Scientific and Technological Development – Brazil, Universal Program grant
349 number 477655/2010-6); it was conducted within an international cooperation agreement
350 between the CNPq (Brazil) and the IRD (Institute for Research and Development – France),
351 and under the auspices of the Environmental Research Observatory Hydrology and
352 Geochemistry of the Amazon Basin (HYBAM), supported by the INSU and the IRD. We are
353 grateful to Jessica Chicheportiche (LOG laboratory) for bacterial abundance estimations. We
354 also want to thanks two anonymous reviewers whose comments helped improve this
355 manuscript.

356

357 **References**

358

359 Abril, G., Martinez, J.M., Artigas, L.F., Moreira-Turcq, P., Benedetti, M.F., Vidal, L.,

360 Meziane, T., Kim, J.H., Bernardes, M.C., Savoye, N., Deborde, J., Souza, E.L.,

361 Alberic, P., Landim de Souza, M.F., Roland, F., 2014. Amazon River carbon dioxide

362 outgassing fuelled by wetlands. *Nature*, 505, 395-398.

363 Alberic, P., 2011. Liquid chromatography/mass spectrometry stable isotope analysis of

364 dissolved organic carbon in stream and soil waters. *Rapid Communications in Mass*365 *Spectrometry*, 25, 3012-3018.

366 Araujo-Lima, C.A.R.M., Forsberg, B.R., Victoria, R., Martinelli L., 1986. Energy sources for

367 detritivorous fishes in the Amazon. *Science*, 234, 1256-1258.

368 Benjamini, Y., Hochberg, Y., 1995. Controlling the false discovery rate: A practical and

369 powerfull approach to multiple testing. *Journal of the Royal Statistical Society Series*370 *B-Methodological*, 57, 289-300.

371 Bligh, E.G., Dyer, W.J., 1959. A rapid method of total lipid extraction and purification.

372 *Canadian Journal of Biochemistry and Physiology*, 37, 911-917.

373 Boschker, H.T.S., de Brouwer, J.F.C., Cappenberg, T.E., 1999. The contribution of

374 macrophyte-derived organic matter to microbial biomass in salt-marsh sediments:

375 Stable carbon isotope analysis of microbial biomarkers. *Limnology and*376 *Oceanography*, 44, 309-319.

377 Bouillon, S., Middelburg, J.J., Dehairs, F., Borges, A.V., Abril, G., Flindt, M.R., Ulomi, S.,

378 Kristensen, E., 2007. Importance of intertidal sediment processes and porewater

379 exchange on the water column biogeochemistry in a pristine mangrove creek (Ras

380 Dege, Tanzania). *Biogeosciences*, 4, 311-322.

381 Chanton, J., Crill, P., Bartlett, K., Martens, C., 1989. Amazon capims (floating grassmats): a

382 source of ¹³C enriched methane to the troposphere. *Geophysical Research Letters*, 16,

383 799-802.

384 Chevaldonne, P., Godfroy, A., 1997. Enumeration of microorganisms from deep-sea

385 hydrothermal chimney samples. *Fems Microbiology Letters*, 146, 211-216.

386 Costantini, M.L., Calizza, E., Rossi, L., 2014. Stable isotope variation during fungal

387 colonisation of leaf detritus in aquatic environments. *Fungal Ecology*, 11, 154-163.

- 388 Devol, A.H., Dossantos, A., Forsberg, B.R., Zaret, T.M., 1984. Nutrient addition experiments
389 in Lago Jacaretinga, Central Amazon, Brazil: 2. The effect of humic and fluvic acids.
390 *Hydrobiologia*, 109, 97-103.
- 391 Ellis, E.E., Richey, J.E., Aufdenkampe, A.K., Krusche, A.V., Quay, P.D., Salimon, C., da
392 Cunha, H.B., 2012. Factors controlling water-column respiration in rivers of the
393 central and southwestern Amazon Basin. *Limnology and Oceanography*, 57, 527-540.
- 394 Engle, D.L., Melack, J.M., 1993. Consequences of riverine flooding for seston and the
395 periphyton of floating meadows in an Amazon floodplain lake. *Limnology and*
396 *Oceanography*, 38, 1500-1520.
- 397 Engle, D.L., Melack, J.M., Doyle, R.D., Fisher, T.R., 2008. High rates of net primary
398 production and turnover of floating grasses on the Amazon floodplain: implications
399 for aquatic respiration and regional CO₂ flux. *Global Change Biology*, 14, 369-381.
- 400 Fellerhoff, C., Voss, M., Wantzen, K.M., 2003. Stable carbon and nitrogen isotope signatures
401 of decomposing tropical macrophytes. *Aquatic Ecology*, 37, 361-375.
- 402 Forsberg, B.R., 1984. Nutrient processing in Amazon floodplain lakes. *Verhandlungen der*
403 *Internationalen Vereinigung für Theoretische und Angewandte Limnologie*, 22,
404 1294-1298.
- 405 Forsberg, B.R., Araujo-Lima, C.A.R.M., Martinelli, L.A., Victoria, R.L., Bonassi, J.A., 1993.
406 Autotrophic carbon sources for fish of the central Amazon. *Ecology*, 74, 643-652.
- 407 Furch, K., Junk, W., 1992. Nutrient dynamics of submersed decomposing Amazonian
408 herbaceous plant species *Paspalum fasciculatum* and *Echinochloa polystachya*. *Revue*
409 *d'hydrobiologie tropicale*, 25, 75-85.
- 410 Grasshoff, K., Kremling, K., Ehrhardt, M., 1999. *Methods of seawater analysis*, Wiley-VCH
411 Verlag GmbH, Weinheim, Germany.
- 412 Hamilton, S.K., Lewis, W.M., Sippel, S.J., 1992. Energy sources for aquatic animals in the
413 Orinoco River floodplain: evidence from stable isotopes. *Oecologia*, 89, 324-330.
- 414 Hedges, J.I., Clark, W.A., Quay, P.D., Richey, J.E., Devol, A.H., Santos, U.D., 1986.
415 Compositions and fluxes of particulate organic material in the Amazon river.
416 *Limnology and Oceanography*, 31, 717-738.
- 417 Hedges, J.I., Cowie, G.L., Richey, J.E., Quay, P.D., Benner, R., Strom, M., Forsberg, B.R.,
418 1994. Origins and processing of organic matter in the Amazon river as indicated by
419 carbohydrates and amino acids. *Limnology and Oceanography*, 39, 743-761.

- 420 Hess, L.L., Melack, J.M., Novo, E.M.L.M., Barbosa, C.C.F., Gastil, M., 2003. Dual-season
421 mapping of wetland inundation and vegetation for the central Amazon basin. *Remote*
422 *Sensing of Environment*, 87, 404-428.
- 423 Howard-Williams, C., Junk, W.J., 1976. The decomposition of aquatic macrophytes in the
424 floating meadows of a Central amazonian varzea lake. In: *Biogeographica*
425 pp. 115-123. The Hague.
- 426 Hubas, C., Artigas, L.F., Davoult, D., 2007a. Role of the bacterial community in the annual
427 benthic metabolism of two contrasted temperate intertidal sites (Roscoff Aber Bay,
428 France). *Marine Ecology Progress Series*, 344, 39-48.
- 429 Hubas, C., Lamy, D., Artigas, L.F., Davoult, D., 2007b. Seasonal variability of intertidal
430 bacterial metabolism and growth efficiency in an exposed sandy beach during low
431 tide. *Marine Biology*, 151, 41-52.
- 432 Johnson, R.W., Calder, J.A., 1973. Early diagenesis of fatty acids and hydrocarbons in a salt-
433 marsh environment. *Geochimica Et Cosmochimica Acta*, 37, 1943-1955.
- 434 Junk, W.J., Howard-Williams, C., 1984. Ecology of aquatic macrophytes in Amazonia. In:
435 *The Amazon, Limnology and Landscape Ecology of a Mighty Tropical River and its*
436 *Basin*. (Ed H. Sioli), pp. 269-293. Junk, Dordrecht.
- 437 Junk, W.J., Piedade, M.T.F., 1993a. Biomass and primary production of herbaceous plant
438 communities in the Amazon floodplain. *Hydrobiologia*, 263, 155-162.
- 439 Junk, W.J., Piedade, M.T.F., 1993b. Herbaceous plants of the Amazon floodplain near
440 Manaus: Species diversity and adaptations to the flood pulse. *Amazoniana-Limnologia*
441 *Et Oecologia Regionalis Systemae Fluminis Amazonas*, 12, 467-484.
- 442 Junk, W.J., Piedade, M.F.T., 1997. Plant life in the floodplain with special reference to
443 herbaceous plants. In: *The central Amazon floodplain: Ecology of a pulsing system*.
444 (Ed W.J. Junk), pp. 147-185. Springer, Berlin Heidelberg New York.
- 445 Kaneda, T., 1991. Iso-fatty and anteiso-fatty acids in bacteria: Biosynthesis, function, and
446 taxonomic significance. *Microbiological Reviews*, 55, 288-302.
- 447 Kern, J., Darwich, A., 2003. The role of periphytic N₂ fixation for stands of macrophytes in
448 the whitewater floodplain (varzea). *Amazoniana-Limnologia Et Oecologia Regionalis*
449 *Systemae Fluminis Amazonas*, 17, 361-375.
- 450 Martinelli, L.A., Victoria, R.L., Trivelin, P.C.O., Devol, A.H., Richey, J.E., 1992. ¹⁵N natural
451 abundance in plants of the Amazon River floodplain and potential atmospheric N₂
452 fixation. *Oecologia*, 90, 591-596.

- 453 Mayorga, E., Aufdenkampe, A.K., Masiello, C.A., Krusche, A.V., Hedges, J.I., Quay, P.D.,
454 Richey, J.E., Brown, T.A., 2005. Young organic matter as a source of carbon dioxide
455 outgassing from Amazonian rivers. *Nature*, 436, 538-541.
- 456 Melack, J.M., Forsberg, B.R., 2001. Biogeochemistry of Amazon floodplain lakes and
457 associated wetlands. In: *The biogeochemistry of the Amazon Basin*. (Eds M.E.
458 McClain & R.L. Victoria & J.E. Richey), pp. 235-274. Oxford University Press, New
459 York.
- 460 Mfilinge, P.L., Meziane, T., Bachok, Z., Tsuchiya, M., 2003. Fatty acids in decomposing
461 mangrove leaves: microbial activity, decay and nutritional quality. *Marine Ecology-
462 Progress Series*, 265, 97-105.
- 463 Moreira-Turcq, P., Bonnet, M.P., Amorim, M., Bernardes, M., Lagane, C., Maurice, L.,
464 Perez, M., Seyler, P., 2013. Seasonal variability in concentration, composition, age,
465 and fluxes of particulate organic carbon exchanged between the floodplain and
466 Amazon River. *Global Biogeochemical Cycles*, 27, 119-130.
- 467 Moreira-Turcq, P., Jouanneau, J.M., Turcq, B., Seyler, P., Weber, O., Guyot, J.L., 2004.
468 Carbon sedimentation at Lago Grande de Curuai, a floodplain lake in the low Amazon
469 region: insights into sedimentation rates. *Palaeogeography Palaeoclimatology
470 Palaeoecology*, 214, 27-40.
- 471 Morison, J.I.L., Piedade, M.T.F., Muller, E., Long, S.P., Junk, W.J., Jones, M.B., 2000. Very
472 high productivity of the C₄ aquatic grass *Echinochloa polystachya* in the Amazon
473 floodplain confirmed by net ecosystem CO₂ flux measurements. *Oecologia*, 125,
474 400-411.
- 475 Mortillaro, J.M., Abril, G., Moreira-Turcq, P., Sobrinho, R., Perez, M., Meziane, T., 2011.
476 Fatty acid and stable isotope ($\delta^{13}\text{C}$, $\delta^{15}\text{N}$) signatures of particulate organic matter in
477 the Lower Amazon River: Seasonal contrasts and connectivity between floodplain
478 lakes and the mainstem. *Organic Geochemistry*, 42, 1159-1168.
- 479 Mortillaro, J.M., Pouilly, M., Wach, M., Freitas, C.E.C., Abril, G., Meziane, T., 2015.
480 Trophic opportunism of central Amazon floodplain fish. *Freshwater Biology*.
481 *Freshwater Biology*, 60, 1659-1670.
- 482 Oksanen, J., Blanchet, F.G., Kindt, R., Legendre, P., O'Hara, R.B., Simpson, G.L., Solymos,
483 P., Stevens, M.H.H., Wagner, H., 2010. Vegan: Community Ecology Package.
484 R package version 1.17-12.
- 485 Peterson, B.J., Fry, B., 1987. Stable isotopes in ecosystem studies. *Annual Review of Ecology
486 and Systematics*, 18, 293-320.

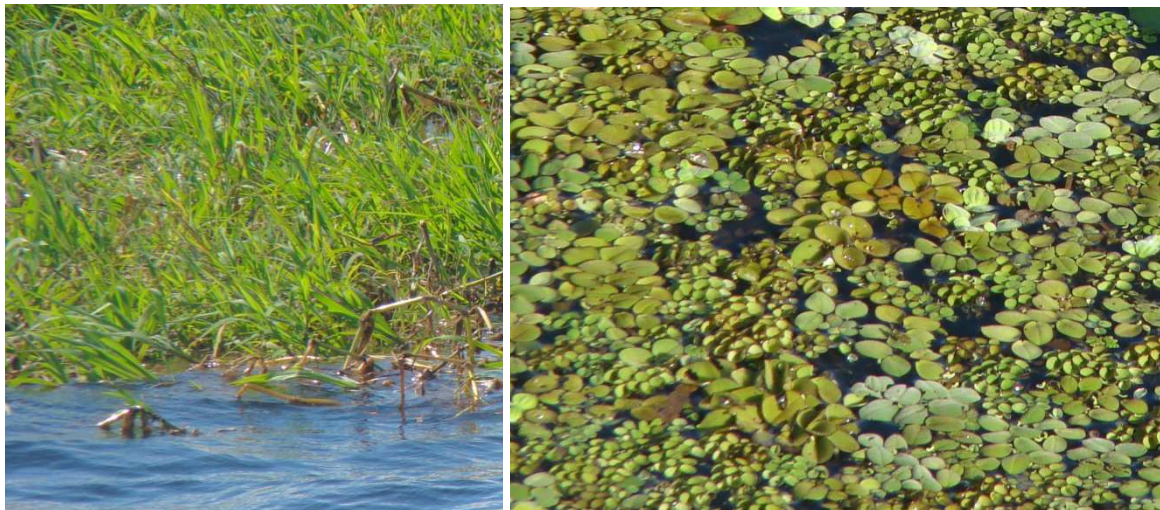
- 487 Piedade, M.T.F., Junk, W.J., Long, S.P., 1991. The productivity of the C₄ grass *Echinochloa*
488 *polystachya* on the Amazon floodplain. *Ecology*, 72, 1456-1463.
- 489 Polsenaere, P., Abril, G., 2012. Modelling CO₂ degassing from small acidic rivers using water
490 pCO₂, DIC and delta C¹³DIC data. *Geochimica Et Cosmochimica Acta*, 91, 220-239.
- 491 Porter, K.G., Feig, Y.S., 1980. The use of DAPI for identifying and counting aquatic
492 microflora. *Limnology and Oceanography*, 25, 943-948.
- 493 Quay, P.D., Wilbur, D.O., Richey, J.E., Hedges, J.I., Devol, A.H., Victoria, R., 1992. Carbon
494 cycling in the Amazon River: Implications from the ¹³C compositions of particles and
495 solutes. *Limnology and Oceanography*, 37, 857-871.
- 496 Rai, H., Hill, G., 1984. Microbiology of Amazonian waters. In: *The Amazon, Limnology and*
497 *Landscape Ecology of a Mighty Tropical River and its Basin*. (Ed H. Sioli),
498 pp. 413-441. Junk, W., Dordrecht.
- 499 Schultz, D.M., Quinn, J.G., 1973. Fatty acid composition of organic detritus from *Spartina*
500 *alterniflora*. *Estuarine and Coastal Marine Science*, 1, 177-190.
- 501 Setaro, F.V., Melack, J.M., 1984. Responses of phytoplankton to experimental nutrient
502 enrichment in an Amazon floodplain lake. *Limnology and Oceanography*, 29,
503 972-984.
- 504 Silva, T.S.F., Costa, M.P.F., Melack, J.M., 2009. Annual net primary production of
505 macrophytes in the Eastern Amazon floodplain. *Wetlands*, 29, 747-758.
- 506 Silva, T.S.F., Melack, J.M., Novo, E., 2013. Responses of aquatic macrophyte cover and
507 productivity to flooding variability on the Amazon floodplain. *Global Change*
508 *Biology*, 19, 3379-3389.
- 509 Smith, B.N., Epstein, S., 1971. Two categories of ¹³C/¹²C ratios for higher plants. *Plant*
510 *Physiology*, 47, 380-384.
- 511 Sobrinho, R.L., Bernardes, M.C., Abril, G., Kim, J.H., Zell, C.I., Mortillaro, J.M., Meziane,
512 T., Moreira-Turcq, P., Sinninghe Damsté, J.S., 2016. Spatial and seasonal contrasts of
513 sedimentary organic matter in floodplain lakes of the central Amazon basin.
514 *Biogeosciences*, 13, 467-482.
- 515 Volkman, J.K., Johns, R.B., Gillan, F.T., Perry, G.J., Bavor, H.J., 1980. Microbial lipids of an
516 intertidal sediment: 1. Fatty acids and hydrocarbons. *Geochimica Et Cosmochimica*
517 *Acta*, 44, 1133-1143.
- 518 Vidal, L.O., Abril, G., Artigas, L.F., Melo, M.L., Bernardes, M.C., Lobão, L.M., Reis, M.C.,
519 Moreira-Turcq, P., Benedetti, M., Tornisiello, V.L., Roland, F., 2015. Hydrological

520 pulse regulating the bacterial heterotrophic metabolism between Amazonian
521 mainstems and floodplain lakes. *Frontiers in microbiology*, 6, 1054.
522 Waichman, A.V., 1996. Autotrophic carbon sources for heterotrophic bacterioplankton in a
523 floodplain lake of central Amazon. *Hydrobiologia*, 341, 27-36.
524 Zuur, A.F., Ieno, E.N., Smith, G.M., 2007. *Analysing Ecological Data*, Springer, Heidelberg,
525 Germany.

526

527

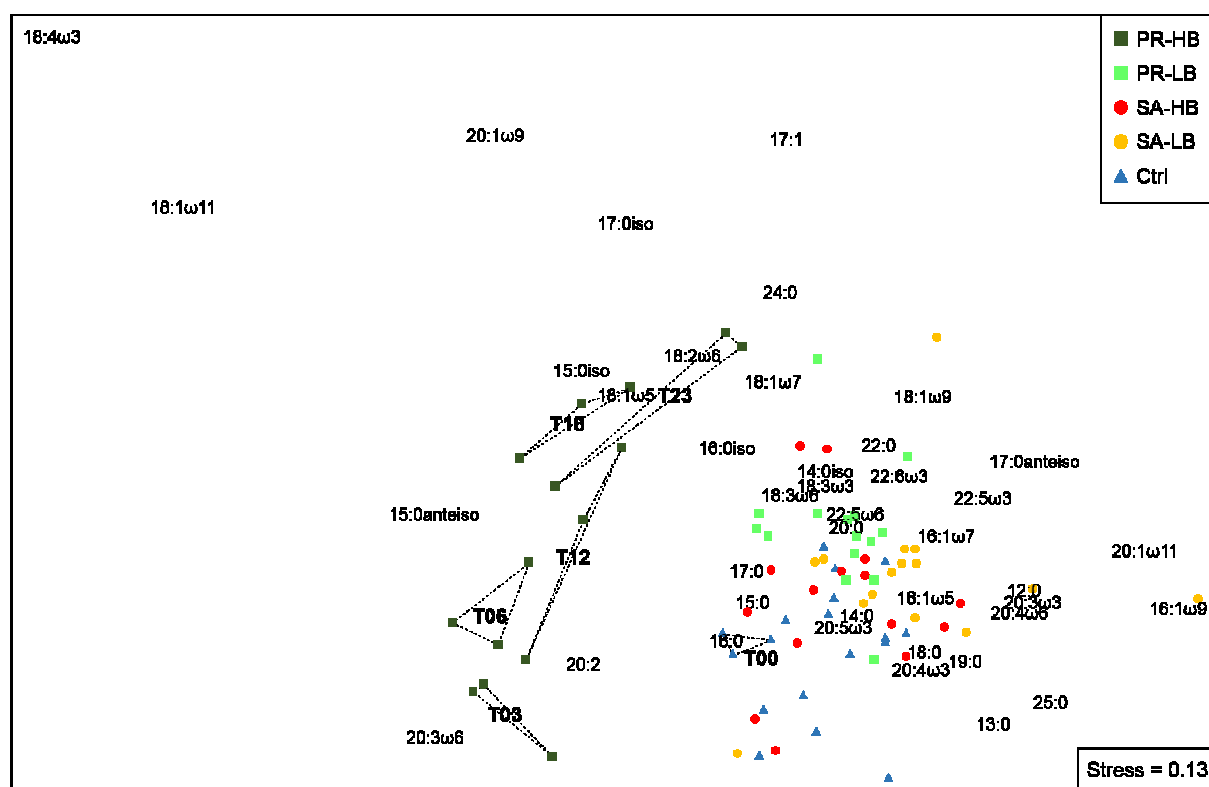
528



529

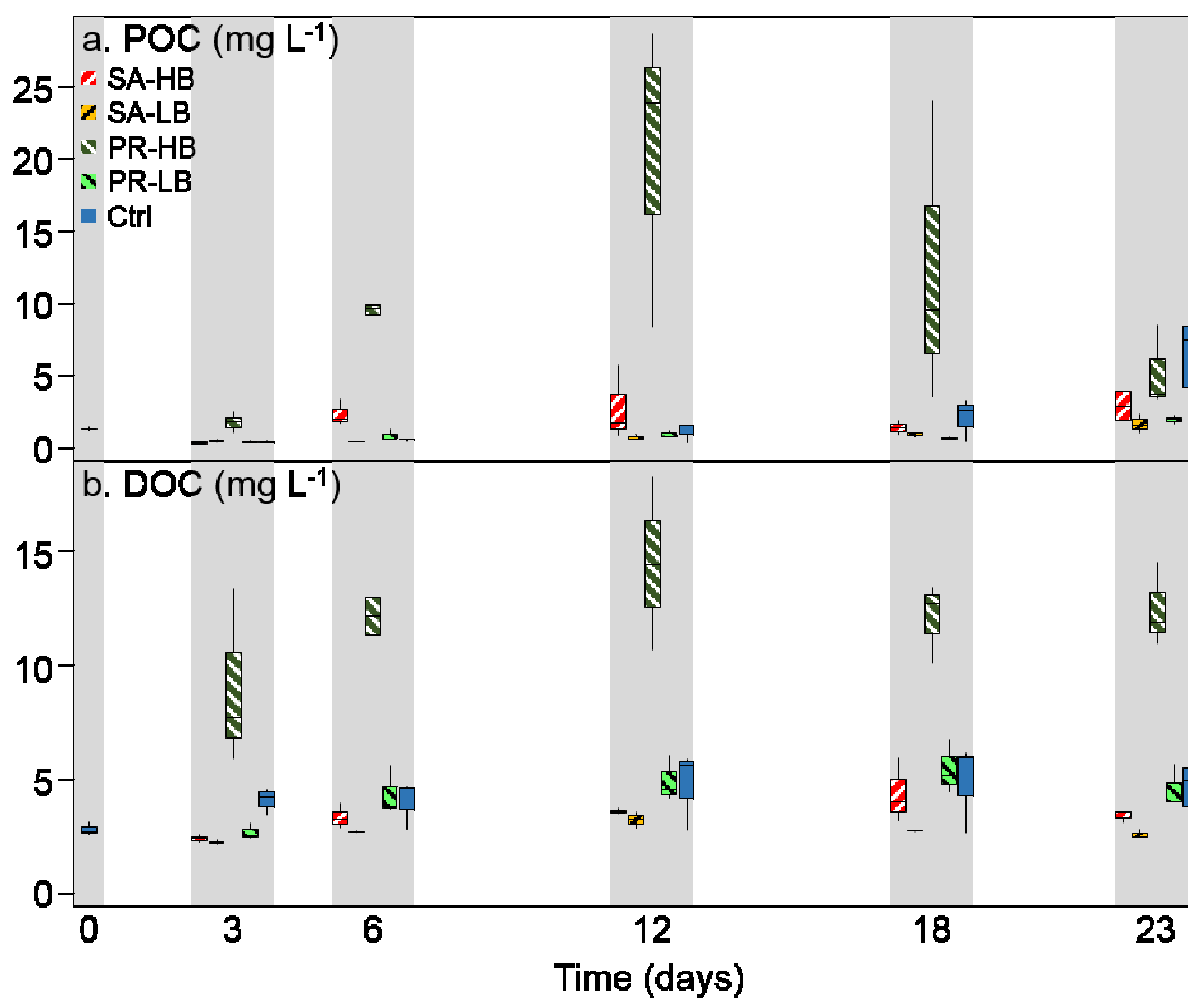
530 Fig. 1. Floating meadows of *P. repens* (left) and *S. auriculata* (right).

531



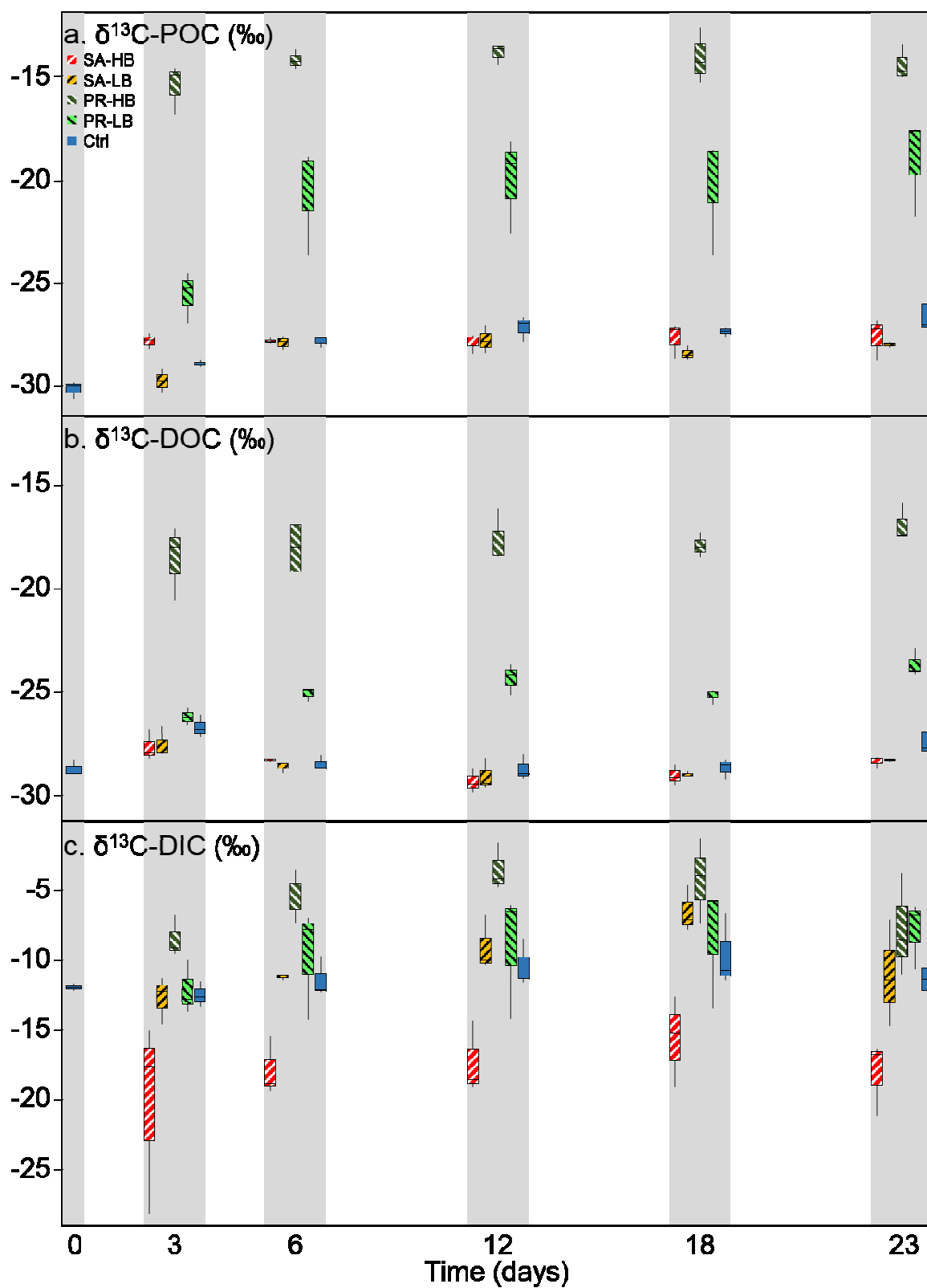
532

533 Fig. 2. Nonmetric MDS of FA proportions (%) in POM. Squares (■) are for *P. repens*
 534 treatments with high (dark green) and low (light green) biomasses, circles (●) are for
 535 *S. auriculata* treatments with high (red) and low (orange) biomasses and blue triangles (▲)
 536 are for the Ctrl treatment.



537

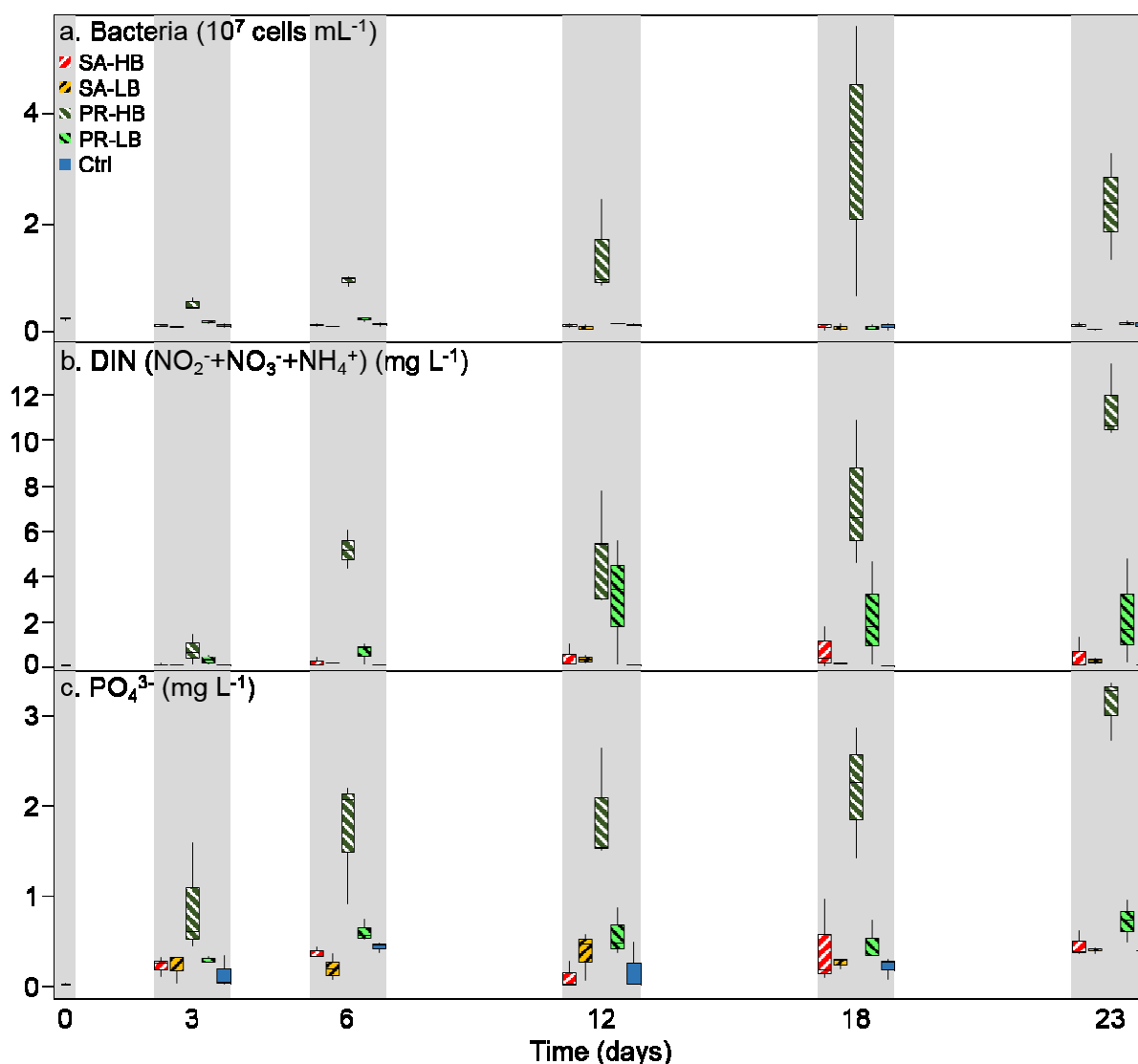
538 Fig. 3. Boxplot of POC (a.) and DOC (b.) concentrations in each treatment: PR-HB (dark
 539 green), PR-LB (light green), SA-HB (red), SA-LB (orange) and Ctrl (blue). Note that DIC
 540 time-courses were not determined because of the CO₂ loss to the atmosphere occurring
 541 throughout the experiment.



542

543 Fig. 4. Boxplot of $\delta^{13}\text{C}$ -POC (a.), $\delta^{13}\text{C}$ -DOC (b.) $\delta^{13}\text{C}$ -DIC (c.) in each treatment: PR-HB

544 (dark green), PR-LB (light green), SA-HB (red), SA-LB (orange) and Ctrl (blue).



545
 546 Fig. 5. Boxplot of bacteria abundances (a.), DIN (b.) and PO_4 (c.) concentrations in each
 547 treatment: PR-HB (dark green), PR-LB (light green), SA-HB (red), SA-LB (orange) and Ctrl
 548 (blue).

549

550

551

552 Table 1. FA concentrations and stable isotope compositions ($\delta^{13}\text{C}$ and $\delta^{15}\text{N}$) of POM
 553 (FA: $\mu\text{g L}^{-1}$) and macrophytes (FA: mg g^{-1}) collected in Camaleão várzea. In bold are the
 554 proportion of saturated (SFA), branched (BFA), monounsaturated (MUFA), polyunsaturated
 555 (PUFA) and long chain FA (LCFA).

	POM ($\mu\text{g L}^{-1}$)	<i>P. repens</i> (mg g^{-1})	<i>S. auriculata</i> (mg g^{-1})
FA	n=3 \pm S.D.	n=3 \pm S.D.	n=3 \pm S.D.
12:0	2.25 \pm 1.81	0.10 \pm 0.02	0.03 \pm 7 10^{-3}
13:0	0.39 \pm 0.10	1 10^{-3} \pm 5 10^{-4}	5 10^{-3} \pm 1 10^{-3}

14:0	6.13 ± 1.61	0.10 ± 4 10 ⁻³	0.20 ± 0.05
15:0	2.25 ± 0.34	0.03 ± 2 10 ⁻³	0.06 ± 0.01
16:0	24.14 ± 3.95	3.69 ± 0.38	2.33 ± 0.28
17:0	0.75 ± 0.10	0.11 ± 0.01	0.05 ± 0.01
18:0	5.54 ± 1.83	0.74 ± 0.12	0.22 ± 0.05
19:0	0.31 ± 0.02	4 10 ⁻³ ± 2 10 ⁻³	7 10 ⁻³ ± 1 10 ⁻³
20:0	0.30 ± 0.09	0.19 ± 0.03	0.02 ± 5 10 ⁻³
22:0	0.38 ± 0.14	0.37 ± 0.07	0.04 ± 4 10 ⁻³
%SFA	78.84 ± 1.76	43.77 ± 4.67	80.35 ± 3.23
14:0iso	0.55 ± 0.13	0.08 ± 0.02	2 10 ⁻³ ± 1 10 ⁻³
15:0anteiso	0.78 ± 0.15	0.05 ± 0.02	0.01 ± 1 10 ⁻³
15:0iso	2.67 ± 0.68	0.06 ± 0.02	0.07 ± 5 10 ⁻³
16:0iso	0.49 ± 0.12	4 10 ⁻³ ± 2 10 ⁻³	0.02 ± 3 10 ⁻³
17:0anteiso	0.58 ± 0.18	3 10 ⁻³ ± 8 10 ⁻⁴	0.01 ± 2 10 ⁻³
17:0iso	0.56 ± 0.13	0.21 ± 0.04	0.04 ± 0.01
%BFA	10.43 ± 0.76	3.23 ± 0.10	3.98 ± 0.18
16:1ω5	0.22 ± 0.03	0.01 ± 4 10 ⁻³	0.02 ± 6 10 ⁻⁴
16:1ω7	0.36 ± 0.32	0.02 ± 5 10 ⁻³	0.01 ± 0.02
16:1ω9	0.13 ± 0.07	0.28 ± 0.11	4 10 ⁻³ ± 3 10 ⁻³
17:1	0.16 ± 0.06	0.01 ± 0.01	0.01 ± 2 10 ⁻³
18:1ω5	0.03 ± 0.00	n.d. ± n.d.	n.d. ± n.d.
18:1ω7	0.10 ± 0.04	0.06 ± 0.01	5 10 ⁻³ ± 6 10 ⁻⁴
18:1ω9	0.01 ± 0.01	n.d. ± n.d.	n.d. ± n.d.
18:1ω9	n.d. ± n.d.	0.21 ± 0.04	2 10 ⁻³ ± 2 10 ⁻³
20:1ω11	n.d. ± n.d.	2 10 ⁻³ ± 5 10 ⁻⁴	n.d. ± n.d.
20:1ω9	n.d. ± n.d.	8 10 ⁻³ ± 3 10 ⁻³	n.d. ± n.d.
%MUFA	1.83 ± 0.35	4.79 ± 0.66	1.30 ± 0.07
16:4ω3	n.d. ± n.d.	0.12 ± 0.02	0.01 ± 4 10 ⁻³
18:2ω6	0.10 ± 0.08	1.34 ± 0.38	2 10 ⁻³ ± 9 10 ⁻⁴
18:3ω3	0.12 ± 0.01	3.60 ± 1.07	0.01 ± 4 10 ⁻³
18:3ω6	0.11 ± 0.06	4 10 ⁻³ ± 1 10 ⁻³	0.08 ± 0.07
18:4ω3	n.d. ± n.d.	n.d. ± n.d.	1 10 ⁻³ ± 2 10 ⁻³
20:2	0.13 ± 0.03	0.01 ± 4 10 ⁻³	4 10 ⁻³ ± 2 10 ⁻³
20:3ω3	0.54 ± 0.26	0.03 ± 0.00	0.01 ± 6 10 ⁻³
20:3ω6	0.31 ± 0.10	0.01 ± 1 10 ⁻³	0.04 ± 0.03
20:4ω3	0.34 ± 0.05	n.d. ± n.d.	3 10 ⁻³ ± 8 10 ⁻⁴
20:4ω6	0.08 ± 0.02	0.02 ± 2 10 ⁻³	3 10 ⁻³ ± 8 10 ⁻⁴
20:5ω3	0.08 ± 0.01	4 10 ⁻³ ± 2 10 ⁻⁴	9 10 ⁻⁴ ± 3 10 ⁻⁴
22:5ω3	0.10 ± 0.04	4 10 ⁻³ ± 1 10 ⁻³	3 10 ⁻³ ± 1 10 ⁻⁴
22:5ω6	2.22 ± 0.43	0.04 ± 6 10 ⁻³	0.05 ± 0.01
22:6ω3	0.39 ± 0.13	0.01 ± 6 10 ⁻⁴	n.d. ± n.d.
%PUFA	8.61 ± 1.67	41.57 ± 4.45	5.68 ± 2.40
24:0	0.05 ± 7 10 ⁻³	0.55 ± 0.11	0.20 ± 0.04
25:0	0.12 ± 0.01	0.04 ± 5 10 ⁻³	0.02 ± 6 10 ⁻³
26:0	n.d. ± n.d.	0.23 ± 0.06	0.10 ± 0.03
%LCFA	0.28 ± 0.02	6.65 ± 0.57	8.69 ± 0.91
δ ¹³ C (‰)	-30.15 ± 0.43	-13.02 ± 0.81	-30.53 ± 0.51
δ ¹⁵ N (‰)	2.43 ± 0.71	4.01 ± 1.32	2.25 ± 1.11

556 n.d. = not detected

557

558 Table 2. Summary of ANOSIM pairwise tests for FA composition of POM between
 559 treatments. Values in italics ($R < 0.3$) are for high intragroup variability.

Groups	<i>R</i>	<i>p</i> value
PR-HB : Ctrl	0.80	$< 10^{-3}$
PR-HB : PR-LB	0.73	$< 10^{-3}$
PR-HB : SA-HB	0.75	$< 10^{-3}$
PR-HB : SA-LB	0.82	$< 10^{-3}$
PR-LB : Ctrl	0.27	$< 10^{-3}$
PR-LB : SA-HB	0.07	0.06 ^{NS}
PR-LB : SA-LB	0.11	$< 10^{-3}$
SA-HB : Ctrl	0.04	0.15 ^{NS}
SA-HB : SA-LB	0.04	0.11 ^{NS}
SA-LB : Ctrl	0.15	0.01

560 NS = non-significant

561 Table 3. Intragroup similarity of FA compositions in different treatments, and percentages of
 562 FA explaining most of this similarity (SIMPER procedure).

Treatment (intragroup similarity)	14:0	15:0iso	15:0anteiso	15:0	16:0	18:0	22:5ω6	Σ (%)
PR-HB (77.3 %)	6.5	11.2	6.3	3.9	44.1	4.9	5.1	76.8
PR-LB (85.1 %)	8.7	6.8	1.6	3.7	33.7	12.7	4.5	73.7
SA-HB (82.6 %)	8.8	3.9	1.5	3.4	37.1	13.8	5.0	75.4
SA-LB (81.7 %)	9.4	3.4	1.4	3.5	33.0	13.2	4.0	71.7
Ctrl (83.7 %)	8.5	3.8	1.4	3.3	39.4	14.3	4.9	77.7

563

564 Table 4. Summary of KW and MWW pairwise tests for $\delta^{13}\text{C}$ -POC, $\delta^{13}\text{C}$ -DOC, $\delta^{13}\text{C}$ -DIC;
 565 POC, DOC, DIN, PO_4^{3-} concentrations and bacterial abundances of water samples between
 566 treatments.

	$\delta^{13}\text{C}$ -POC	$\delta^{13}\text{C}$ -DOC	$\delta^{13}\text{C}$ -DIC	[POC]	[DOC]	[DIN]	$[\text{PO}_4^{3-}]$	Bact
KW Global test	$5 \cdot 10^{-7}$	$3 \cdot 10^{-8}$	$6 \cdot 10^{-9}$	$5 \cdot 10^{-6}$	$4 \cdot 10^{-6}$	10^{-5}	10^{-6}	10^{-9}
PR-HB : Ctrl	$7 \cdot 10^{-4}$	$3 \cdot 10^{-4}$	$8 \cdot 10^{-4}$	$1 \cdot 10^{-3}$	$1 \cdot 10^{-3}$	$1 \cdot 10^{-3}$	$2 \cdot 10^{-3}$	$< 10^{-4}$
PR-HB : PR-LB	$7 \cdot 10^{-4}$	$1 \cdot 10^{-3}$	0.03	$1 \cdot 10^{-4}$	$1 \cdot 10^{-3}$	0.05	$5 \cdot 10^{-3}$	$< 10^{-4}$
PR-HB : SA-HB	$7 \cdot 10^{-4}$	$2 \cdot 10^{-4}$	$< 10^{-4}$	$7 \cdot 10^{-3}$	$1 \cdot 10^{-3}$	$4 \cdot 10^{-3}$	$2 \cdot 10^{-3}$	$< 10^{-4}$
PR-HB : SA-LB	$7 \cdot 10^{-4}$	$2 \cdot 10^{-4}$	$9 \cdot 10^{-3}$	$1 \cdot 10^{-4}$	$2 \cdot 10^{-4}$	$4 \cdot 10^{-3}$	$2 \cdot 10^{-3}$	$< 10^{-4}$
PR-LB : Ctrl	$9 \cdot 10^{-4}$	$3 \cdot 10^{-4}$	0.44 ^{NS}	0.86 ^{NS}	0.71 ^{NS}	$2 \cdot 10^{-3}$	0.07 ^{NS}	0.15 ^{NS}
PR-LB : SA-HB	$7 \cdot 10^{-4}$	$2 \cdot 10^{-4}$	$< 10^{-4}$	0.05	0.06 ^{NS}	0.09 ^{NS}	0.06 ^{NS}	0.06 ^{NS}
PR-LB : SA-LB	$7 \cdot 10^{-4}$	$2 \cdot 10^{-4}$	0.59 ^{NS}	0.64 ^{NS}	$2 \cdot 10^{-3}$	0.13 ^{NS}	0.06 ^{NS}	0.01
SA-HB : Ctrl	0.60 ^{NS}	0.23 ^{NS}	$< 10^{-4}$	0.29 ^{NS}	0.11 ^{NS}	0.06 ^{NS}	0.90 ^{NS}	0.33 ^{NS}
SA-HB : SA-LB	0.11 ^{NS}	0.94 ^{NS}	$< 10^{-4}$	0.03	0.02	0.46 ^{NS}	0.90 ^{NS}	0.12 ^{NS}
SA-LB : Ctrl	0.08 ^{NS}	0.25 ^{NS}	0.38 ^{NS}	0.58 ^{NS}	$2 \cdot 10^{-3}$	$1 \cdot 10^{-3}$	0.90 ^{NS}	0.04

567 NS = non-significant.

568